



Research article

UDC 691.43

DOI: 10.34910/MCE.121.4



## High-strength building ceramics based on fly ash – red mud mixtures

T. Vakalova , N. Sergeev , D. Tolegenov , D. Tolegenova

National Research Tomsk Polytechnic University, Tomsk, Russian Federation

✉ [tvv@tpu.ru](mailto:tvv@tpu.ru)

**Keywords:** fly ash, red mud, sintering, mechanical strength, anorthite, building ceramics

**Abstract.** The work is devoted to the actual problem of creating high-strength ceramic materials based on technogenic waste. This problem is solved by using low-calcium (2.26 % CaO) aluminosilicate fly ash from the combustion of solid fuel (coal) as the main raw material component with the additions of high-iron (22–25 % Fe<sub>2</sub>O<sub>3</sub> in the calcined state) bauxite sludge. The chemical and mineralogical features of the initial fly ash and bauxite sludge, as well as their structural and phase changes during heating were studied. The predictive analysis of the behavior of ash and bauxite sludge mixtures in the CaO–Al<sub>2</sub>O<sub>3</sub>–SiO<sub>2</sub>, Fe<sub>2</sub>O<sub>3</sub>–Al<sub>2</sub>O<sub>3</sub>–SiO<sub>2</sub>, and FeO–Al<sub>2</sub>O<sub>3</sub>–SiO<sub>2</sub> systems made it possible to identify the fluxing effect of bauxite sludge additions to fly ash. The main criteria for designing compositions (Fe<sub>2</sub>O<sub>3</sub>/Al<sub>2</sub>O<sub>3</sub> and CaO/SiO<sub>2</sub> modules) of ceramic masses based on ash and sludge for the production of high-strength ceramics are proposed. The iron-alumina module is responsible for the formation of the melt; the calcium silicate module is responsible for the formation of the crystalline phase (anorthite) during firing. The established sintering-hardening effect of bauxite sludge additives in an amount of 10–25 % in compositions with fly ash provides a 1.7–2-fold increase in the compressive strength of samples of semi-dry pressing (from 95 to 206 MPa) at firing temperatures of 1200 °C. The recommended compositions are promising for obtaining densely sintered calcium aluminosilicate building ceramics (paving stones, porcelain stoneware, clinker bricks) with a predominantly anorthite crystalline phase with a water absorption of 0.5–2 % and a compressive strength of up to 175–200 MPa.

**Acknowledgements:** The research was carried out using the equipment of the CSU NMNT TPU, supported by the RF MES project No. 075-15-2021-710.

**Citation:** Vakalova, T., Sergeev N., D. Tolegenov, D. Tolegenova. High-strength building ceramics based on fly ash – red mud mixtures. Magazine of Civil Engineering. 2023. 121(5). Article no. 12104. DOI: 10.34910/MCE.121.4

### 1. Introduction

The large-scale production of traditional ceramic materials (porcelain, faience, sanitary ceramics, building ceramics, etc.) is accompanied by active consumption of high-quality natural raw materials, leading to a gradual decrease in their reserves. There is a need to expand the scope of the use of non-standard natural raw materials, as well as industrial waste to obtain modern ceramic materials with improved physical and mechanical properties (mechanical strength, frost resistance, chemical resistance, etc.).

Pollution of industrial solid waste has become an increasingly serious problem. Every year, large quantities of metallurgical wastes are generated from the production of various metals. These residues are considered as hazardous wastes due to their soluble metal content, which induces many social problems

such as contaminated water, dust-laden air and alkalized soils, as well as human and animal health and security risks from the disintegration of wastes. For example, worldwide, the alumina industry produces approximately 70 Mt/annum of hazardous bauxite residue (so-called “red mud”) [1, 2]. Typically, red mud is considered as a waste discharged to sea, in ponds or landfills. Moreover, discharge of red mud is environmentally hazardous because of its alkalinity [3]. Many studies have been conducted to develop the uses of red mud. It is widely accepted that using red mud as ceramics and building materials is the most promising approach because of its tremendous consumption [4–12].

Fly ash is generated during the combustion of pulverized coal from thermal power plants. It has been posing a heavy problem to the environment and economic growth throughout the world, since it is utilized much less today than generated [13–15]. Coal fly ash is one of the most complex materials to characterize. Approximately 316 individual minerals and 188 mineral groups have been identified in various fly ash samples [16, 17]. The major components are metallic oxides with varying contents of unburnt carbon as measured by a loss on ignition test. The contents of principal oxides are usually in a descending order:  $\text{Al}_2\text{O}_3$ . Construction industry is still its chief consumer, but its products including bricks, expanded clay, cement and concrete are generally of low value [18–23]. Recently, increased attention has been focused on how fly ash is utilized in the high-value products, such as high-strength mullite ceramics [24–27], cordierite ceramics and cordierite glass-ceramics [28, 29], anorthite-based ceramics [30, 31],  $\text{Al}_2\text{O}_3$ -SiC composite materials [32], zirconia–mullite–corundum ceramics [33], zeolite-containing adsorbents for wastewater treatment and radioactive waste immobilization [34].

It is known that the mechanical strength of ceramics primarily depends on its phase composition — the content of the crystalline and glassy phases: the greater the amount of the crystalline phase, the greater the strength [35]. The nature of crystalline phases, the conditions of their formation, the habit of its particles are important for the formation of the mechanical properties of ceramics too. In particular, if the crystals are elongated (for example, particles of acicular mullite or wollastonite), then the strength of ceramics will increase due to the formation of a crystalline framework [36, 37]. If the formation of the crystalline phase occurs with volumetric changes (for example, the transition of quartz to cristobalite), this can lead to an increase in porosity and to a decrease in strength [35]. However, if the content effect of the glass phase and the crystalline phase on the mechanical strength of the ceramic is compared, then an increase in the total content of the crystalline phase and, accordingly, a decrease in the amount of glass phase in the composition of the ceramic material will enhance its strength. On the other hand, the mechanical strength also depends on the degree of sintering behavior (density or porosity) [38]. Therefore, to increase the strength of the ceramic material, it is necessary to reduce its overall porosity and/or to increase the content of the crystalline phase.

The possibility of using fly ash and bauxite sludge as a raw material for obtaining building ceramics with improved functional properties is determined by the proximity of the chemical composition of the waste and traditional ceramic raw materials (clays, kaolins, silica raw materials, etc.).

Thus, the involvement of technogenic waste in the production of ceramic materials will reduce the need for primary mineral resources. There will be no need for specialized quarries to extract natural raw materials, disturb natural landscapes, etc. Utilization of waste from mining and metallurgical, fuel and energy industries in the silicate materials industry will allow solving not only environmental, but also economic problems, since raw materials from waste for the production of ceramics are 2–3 times cheaper than natural ones.

The purpose of this work is to determine the technological parameters for the creation of high-strength building ceramics based on fly ash from the combustion of solid fuels using red mud as a sintering and hardening additive.

To achieve this objective, it is necessary to solve the following tasks:

- to establish the chemical composition, mineralogical (phase) composition, structural features of the initial technogenic raw materials (fly ash and bauxite sludge);
- to study their (fly ash and bauxite sludge) structural and phase changes during heating;
- to carry out theoretical and exploratory research on the development of compositions and technological parameters for the obtaining of high-strength ceramic materials based on man-made waste.

## 2. Methods

### 2.1. Characteristics of initial raw materials used

According to the chemical composition, the studied fly ash is a kind of acid ash with a low content of calcium oxide (2.26 % CaO) and a high content of aluminum oxide (29.19 %  $\text{Al}_2\text{O}_3$ ) and iron oxide (12.11 %  $\text{Fe}_2\text{O}_3$ ) in the calcined state (Table 1).

**Table 1. Chemical composition of the investigated raw materials.**

Raw materials	Content of oxides, wt. %									
	$\text{SiO}_2$	$\text{Al}_2\text{O}_3$	$\text{TiO}_2$	$\text{Fe}_2\text{O}_3$	MnO	CaO	MgO	$\text{K}_2\text{O}$	$\text{Na}_2\text{O}$	LOI
fly ash										
Absolutely dry state	47.37	28.49	0.96	11.82	2.65	2.19	3.35	0.42	0.35	2.39
Calcined state*	48.53	29.19	0.99	12.11	2.71	2.26	3.43	0.43	0.35	-
red mud										
Absolutely dry state	21.03	7.47	2.16	17.27	1.12	23.46	2.33	0.31	0.43	24.37
Calcined state*	27.88	9.88	2.86	22.83	1.48	31.02	3.08	0.41	0.57	-

\* – after calcination at 950 °C

Red mud in the initial state is characterized by high values of mass loss upon ignition (up to 24.37 %), which can complicate its use in the technological process of obtaining molded ceramic materials. In the calcined state, the chemical composition of red mud is dominated by the content of calcium oxide (31.02 % CaO), iron oxide (22.83 %  $\text{Fe}_2\text{O}_3$ ) and silicon oxide (27.88 %  $\text{SiO}_2$ ), which account for up to 80 % (81.73 %) of the total content all oxides (Table 1).

X-ray analysis of the fly ash indicates that the investigated fly ash in the initial state is a material with a significant content of glass phase, as evidenced by the presence of an intense diffuse background in the X-ray diffraction pattern (Fig. 1).

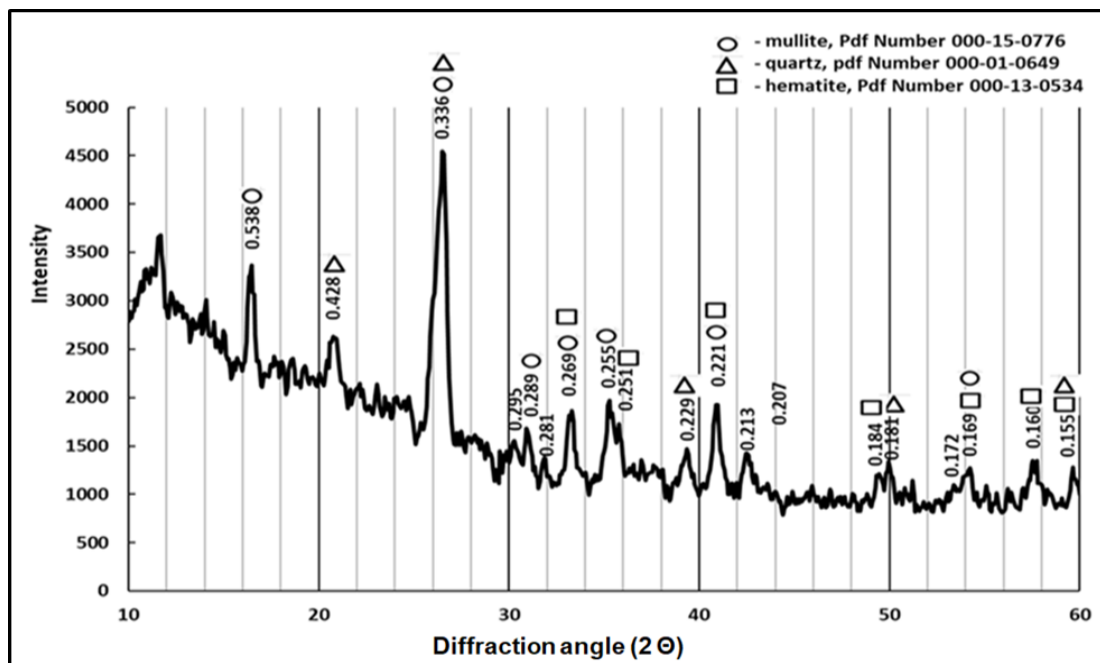


**Figure 1. X-ray diffraction pattern of the initial fly ash.**

The crystalline part of the fly ash is composed of mullite ( $d_a/n - 0.538, 0.336, 0.289, 0.269, 0.255, 0.221$  nm, etc.), quartz ( $d_a/n - 0.428, 0.336, 0.229, 0.212, 0.181$  nm, etc.) and iron mineral in the form of hematite ( $d_a/n - 0.269, 0.251, 0.219, 0.183$  nm, etc.).

A comparative analysis of the data of chemical analysis (Table 1) and X-ray method (Fig. 2) indicates that the calcium component in the red mud is presented in the form of calcite  $\text{CaCO}_3$ , as evidenced by X-ray reflections with  $d_a/n - 0.303, 0.250, 0.209, 0.187$  nm, etc., also in the form of hydrated silicates and aluminates calcium: dicalcium hydrosilicate  $\gamma - 2\text{CaO} \cdot \text{SiO}_2 \cdot \text{H}_2\text{O}$  ( $d_a/n - 0.383, 0.270, 0.189$  nm), as well as hexacalcium tricarbonat hydroaluminat  $3\text{CaO} \cdot \text{Al}_2\text{O}_3 \cdot 3\text{CaCO}_3 \cdot 32\text{H}_2\text{O}$  ( $d_a/n - 0.383, 0.270, 0.251$  nm, etc.). The iron component is represented by hematite  $\text{Fe}_2\text{O}_3$  ( $d_a/n - 0.270, 0.252, 0.220, 0.184$  nm) and magnetite  $\text{Fe}_3\text{O}_4$  ( $d_a/n - 0.297, 0.252, 0.209, 0.161$  nm).

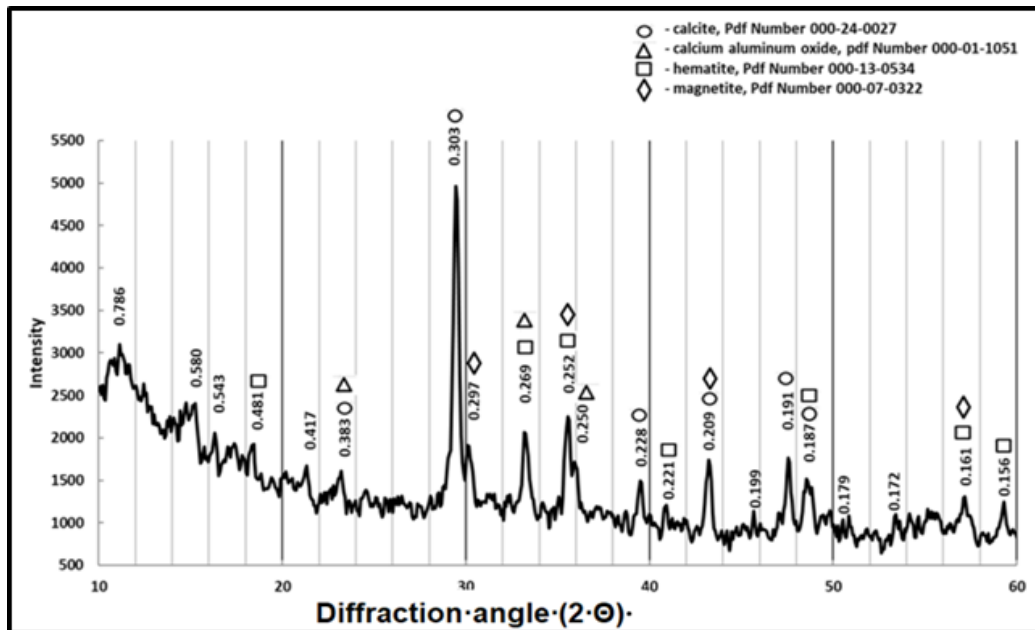
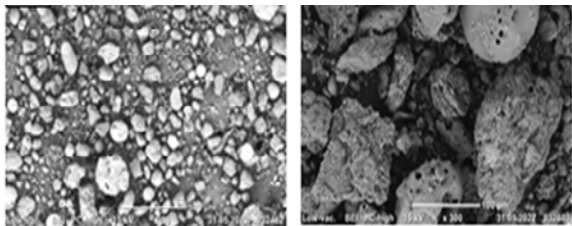
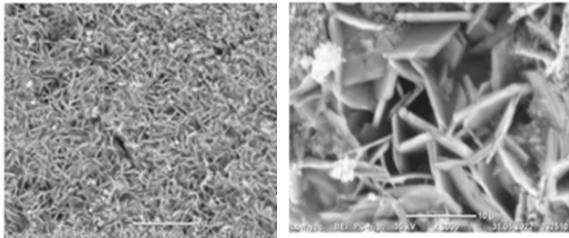


Figure 2. X-ray diffraction pattern of red mud.

According to electron microscopy data, fly ash in the initial state consists of sintered conglomerates of isometric and elongated shapes and rounded particles close to the shape of a sphere (Table 2).

Table 2. Microstructure and dispersion of raw materials.

Raw materials	Microstructure	Particle shape and size
Fly ash		<ol style="list-style-type: none"> <li>1) round-shaped particles ranging in size from 25 to 95–100 μm,</li> <li>2) sintered aggregates of isometric shape from 150 to 250 μm,</li> <li>3) non-metric aggregates 70–100 μm long and 20–30 μm wide.</li> </ol>
Red mud		lamellar crystals 11.8 to 15.7 μm long and up to 2 μm thick.

Fly ash microspheres have a hollow structure and a melted surface with numerous sintered particles. The agglomerates have a densely sintered structure with a small number of pores on the surface of the particles. Bauxite sludge is composed of lamellar crystals intertwined with each other.

## 2.2. Procedures and methods

The study of the behavior of fly ash and red mud upon heating was carried out on specimens in the form of tablets with a diameter of 20 mm (3 samples per temperature) and cylinders 20×20 mm (8 samples per temperature). They were formed from fine powder (less than 0.063 mm) by semi-dry pressing using a 1 % solution of carboxymethylcellulose as a binder. The required degree of compaction of the press powder and the pressure required for this were selected empirically. The specific pressure was varied from 10 to 30 MPa with an interval of 5 MPa, with holding at maximum pressure for 10 sec. The optimum pressing pressure was 20 MPa (based on the maximum bulk density of the compacts). The samples were dried to an air-dry state, after which they were fired in the range of 950–1150 °C with an interval of 50 °C and holding at the final temperature for 2 h. The calcined samples were cooled together with a furnace in a free mode.

The influence of red mud additives in the amount of 10–25 wt.% on mineral formation processes and sintering processes of mixtures with fly ash was assessed on 20×20 mm cylinder samples (5 samples per temperature). The samples were molded by the semi-dry pressing at the pressure of 20 MPa. For this, red mud was pre-calcined at 1100 °C in order to remove chemically bound water and synthesize new crystalline phases in raw materials, and not in molded samples. The fly ash was also pre-calcined at a temperature of 1200 °C to crystallize the glass phase of the fly ash when heated into cristobalite in raw materials, since the formation of cristobalite adversely affects the mechanical properties of the fired samples. Then, mixtures of calcined fly ash and red mud were ground by dry method in a ball mill with a high alumina ceramic lining and grinding balls until the particles completely pass through a 0063 sieve (250 mesh). Sintering of pressed samples was carried out at a temperature of 1200–1300 °C with a heating rate of 1.5 °C/min and an exposure at maximum temperature for 2 hours.

## 2.3. Experimental method

The physicochemical and processing properties of the initial fly ash and red mud upon heating, the studied mixtures of fly ash with red mud additives and finished products were investigated using physical and chemical methods. These methods include traditional chemical and elemental analyses by an Oxford XSupreme 8000 X-ray fluorescence analyzer. The phase compositions of the specimens were analyzed via an X-ray diffractometer (Shimadzu XRD-7000S) with CuK $\alpha$  radiation ( $\lambda K\alpha = 0.154186$  nm) at 40 kV and 25 mA. The specimens were tested in the angle range of 10–60° (2 $\theta$ ). Moreover, the crystalline phases were identified on the basis of the experimental patterns using the Powder Diffraction File Database of the International Center for Diffraction Data. The microstructures were observed using a scanning electron microscope (Hitachi S-570 and JEOL JSM-840). A thermal analysis was carried out to study the thermal behavior of the rock used up to 1000 °C at a heating rate of 10 °C/min (TG/DSC/DTA thermal analyzer with an SDTQ 60 mass spectrometer).

Air and fire shrinkage was determined on the tablet samples. Sample drying shrinkage were measured by controlling sample length, width and height before and after drying process.

The measurements of water absorption were performed via the Archimedes method. The compressive strength of the fired samples was measured by using cubic samples. The reported compressive strength (MPa) is the average of five measurements.

## 3. Results and Discussion

### 3.1. Characteristic of phase changes during heating of the fly ash and red mud used

The use of fly ash and red mud as raw materials for the production of ceramics makes it necessary to study their behavior when heated.

When comparing the X-ray diffraction patterns of the initial ash and the ash fired at 1000 °C, a decrease in the intensity and area of the diffuse background is noted, which indicates a decrease in the content of the glass phase in the fly ash during its heating (Fig. 3). This causes the appearance on the X-ray diffraction pattern of fired fly ash of a low-intensity characteristic reflection of cristobalite SiO<sub>2</sub> with an interplanar distance of  $d_a/n - 0.411$  nm, while the intensity of the characteristic reflection of quartz remains unchanged ( $d_a/n - 0.427$  nm). The formation of cristobalite nuclei in fly ash at 1000 °C is caused by the crystallization of the glass phase, which leads to a decrease in the area of the diffuse background.

In addition to the appearance of cristobalite at 1000 °C, the formation of another new crystalline phase, anorthite  $\text{CaO} \cdot \text{Al}_2\text{O}_3 \cdot 2\text{SiO}_2$  was recorded, as evidenced by the appearance of a low-intensity reflex with  $d_a/n = 0.320$  nm.

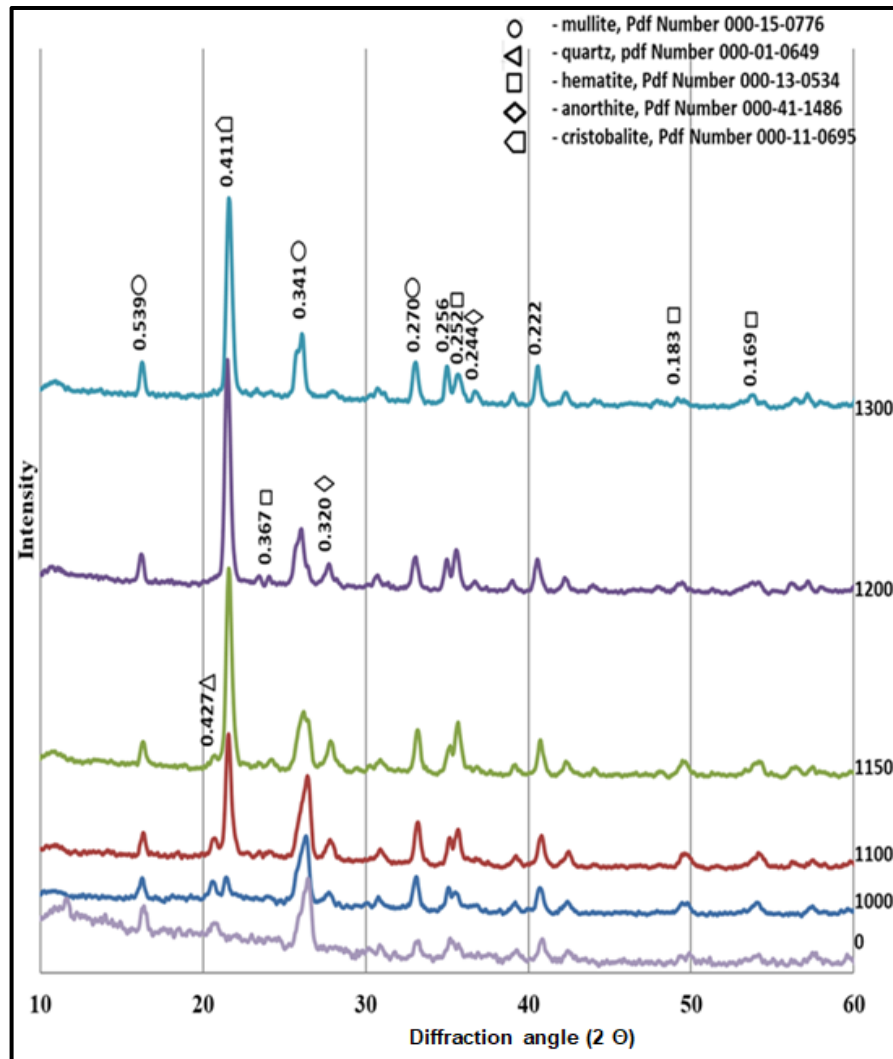


**Figure 3. X-ray diffraction patterns of fly ash fired at 1000–1300 °C.**

A further increase in the firing temperature from 1000 to 1300 °C has practically no effect on the change in the diffraction pattern of the firing products of the fly ash samples. The difference consists only in the change in the intensity of X-ray reflections. In particular, the height of mullite reflections increases, which may be due to both an increase in the content of mullite and the processes of improving its crystal structure, or both reasons simultaneously. X-ray reflexes of cristobalite grow sharply, which indicates an increase in its content. The intensity of anorthite reflections (0.320, 0.249 nm) increases, although to a lesser extent than for mullite and cristobalite. As for hematite  $\text{Fe}_2\text{O}_3$ , the mineral component of the initial fly ash, with an increase in temperature up to 1300 °C, its reflections are preserved with a slight decrease in their intensity (0.251, 0.183, 0.169 nm). This may be due to the participation of hematite in the formation of an iron silicate melt during the firing of the initial fly ash at temperatures of 1000–1300 °C.

Thus, the mineralogical composition of the crystalline part of the studied fly ash, fired at 1000–1300 °C, is represented by the initial minerals – mullite  $3\text{Al}_2\text{O}_3 \cdot 2\text{SiO}_2$  and hematite  $\text{Fe}_2\text{O}_3$ , as well as new phases formed during the firing process – cristobalite  $\text{SiO}_2$  and anorthite  $\text{CaO} \cdot \text{Al}_2\text{O}_3 \cdot 2\text{SiO}_2$  (Table 3).

**Table 3. Change in the phase composition of the investigated fly ash after firing at 1000–1300 °C.**

Phase	Formula	Presence*		Processes during heating of ash
		in the initial ash	after firing at 1000–1300 °C	
mullite	$3\text{Al}_2\text{O}_3 \cdot 2\text{SiO}_2$	+	++	
quartz	$\text{SiO}_2$	+	--	quartz → cristobalite
hematite	$\text{Fe}_2\text{O}_3$	++	+	hematite (partially) → melt
glass phase		+++	+	glass phase (partially) → cristobalite
cristobalite	$\text{SiO}_2$	--	+	
anorthite	$\text{CaO} \cdot \text{Al}_2\text{O}_3 \cdot 2\text{SiO}_2$	--	+	

\* + present, -- absent

An assessment of the physical and mechanical properties of samples of semi-dry pressing from finely ground initial fly ash, fired in the temperature range of 1000–1300 °C (Fig. 4), indicates that the highest compressive strength (94 MPa) is achieved at a temperature of 1300 °C (water absorption 10.2 %). Therefore, to exceed the mechanical compressive strength of 95 MPa in the samples of semi-dry pressing, it is necessary to activate the sintering process of the studied fly ash.

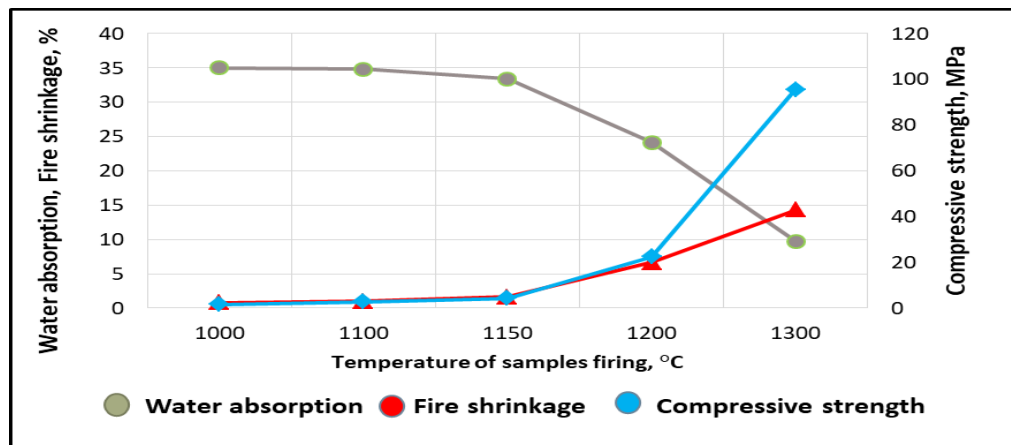


**Figure 4. Effect of heating temperature on changes in fire shrinkage, water absorption and compressive strength in the samples made of the studied fly ash.**

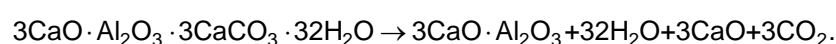
This can be done in different ways: by preliminary heat treatment of aluminosilicate fly ash, by increasing the firing temperature above 1300 °C, by selecting sintering additives. Previously, the authors revealed the effect of various oxide additives on the sintering process of aluminosilicate ceramics, including iron additives [39]. The studied bauxite sludge contains a high content of iron oxide ( $22.8 \text{ Fe}_2\text{O}_3$ ) and may be promising for activating the sintering of aluminosilicate fly ash samples.

According to X-ray studies, the thermal treatment of red mud in the temperature range of 900–1100 °C is accompanied by complex physical and chemical processes, already starting from 900 °C. This leads to a change in the X-ray diffraction patterns of fired red mud samples compared to the initial red mud (Fig. 5):

1. The decrease of the diffuse background in the low-angle region is associated with a decrease in the content of the amorphous phase of red mud due to the crystallization of its components upon heating.

2. Complete decarbonization of calcite  $\text{CaCO}_3$ , which manifests itself in the disappearance of the main calcite reflections with interplanar distances of 0.303, 0.250, 0.209, 0.187 nm in the X-ray diffraction patterns.

3. The disappearance of reflections at 0.383, 0.270, 0.250 nm and the appearance of intense reflections at 0.276 and 0.270 nm, as well as less intense reflections at 0.511, 0.424, 0.245, 0.220 nm, are due to the process of dehydration and decarbonization of hexacalcium tricarbonat hydroaluminat  $3\text{CaO} \cdot \text{Al}_2\text{O}_3 \cdot 3\text{CaCO}_3 \cdot 32\text{H}_2\text{O}$  to tricalcium aluminate  $3\text{CaO} \cdot \text{Al}_2\text{O}_3$ :



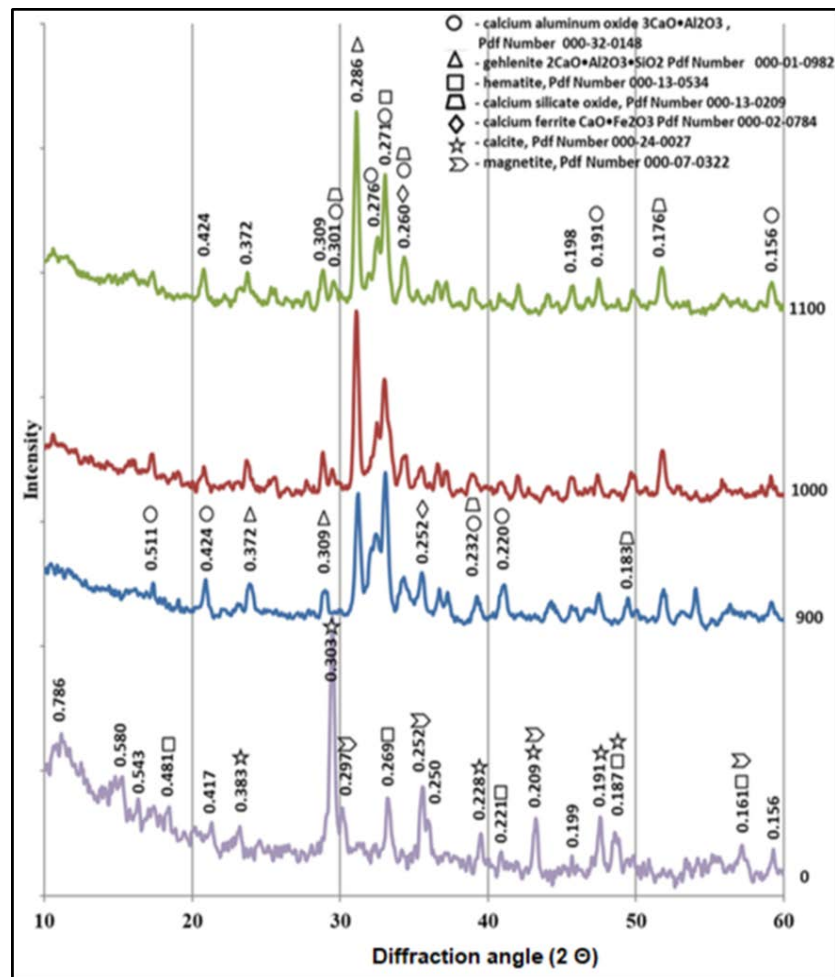


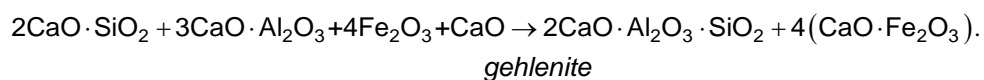
Figure 5. X-ray diffraction patterns of red mud fired at 900–1100 °C.

The presence of calcium aluminum oxide, also found by other authors [11, 40], is consistent with most XRD spectra and is likely in view of the availability of CaO and Al<sub>2</sub>O<sub>3</sub> in the chemical composition of red mud.

4. The appearance of an intense reflection at 0.286 nm, as well as reflections at 0.372, 0.307, 0.245, 0.241, 0.204 nm indicate the synthesis of a new crystalline phase in the form of gehlenite 2CaO·Al<sub>2</sub>O<sub>3</sub>·SiO<sub>2</sub>.

An increase in the firing temperature of the red mud from 900 to 1100 °C practically does not change the diffraction pattern of the fired products. The difference consists only in a decrease in the intensity of reflections of tricalcium aluminate 3CaO·Al<sub>2</sub>O<sub>3</sub>, a decrease in the intensity of reflections of hematite Fe<sub>2</sub>O<sub>3</sub>, and an increase in the intensity of reflections of gehlenite 2CaO·Al<sub>2</sub>O<sub>3</sub>·SiO<sub>2</sub>.

The recorded changes make it possible to determine the reaction for the synthesis of gehlenite at a temperature within the 900–1100 °C range:



The formation of monocalcium ferrite at temperatures of 900–1100 °C along with gehlenite is indicated by the appearance of its reflexes ( $d_a/n$  - 0.261, 0.252, 0.227, 0.215, 0.184 nm) on the X-ray diffraction patterns.

Thus, the mineralogical composition of the crystalline part of red mud fired at 900–1100 °C is represented by tricalcium aluminate 3CaO·Al<sub>2</sub>O<sub>3</sub>, hematite Fe<sub>2</sub>O<sub>3</sub>, gehlenite 2CaO·Al<sub>2</sub>O<sub>3</sub>·SiO<sub>2</sub> and monocalcium ferrite CaO·Fe<sub>2</sub>O<sub>3</sub> (Table 4).



**Table 4. Change in the phase composition of the investigated red mud firing at 900–1100 °C.**

Phase	Formula	Presence*		Processes during heating of red mud
		in the initial red mud	after firing at 900–1100 °C	
calcite	$\text{CaCO}_3$	+	--	$\text{CaCO}_3 \rightarrow \text{CaO}$
dicalcium hydrosilicate	$2\text{CaO} \cdot \text{Al}_2\text{O}_3 \cdot \text{SiO}_2$	+	--	$2\text{CaO} \cdot \text{SiO}_2 \cdot \text{H}_2\text{O} \rightarrow 2\text{CaO} \cdot \text{SiO}$
hexacalcium tricarbonat hydroaluminate	$3\text{CaO} \cdot \text{Al}_2\text{O}_3 \cdot 3\text{CaCO}_3 \cdot 32\text{H}_2$	+	--	$3\text{CaO} \cdot \text{Al}_2\text{O}_3 \cdot 3\text{CaCO}_3 \cdot 32\text{H}_2\text{O} \rightarrow 3\text{CaO} \cdot \text{Al}_2\text{O}_3 \cdot 3\text{CaO}$
magnetite	$\text{Fe}_3\text{O}_4$	+	--	$\text{Fe}_3\text{O}_4 \rightarrow \text{Fe}_2\text{O}_3$
hematite	$\text{Fe}_2\text{O}_3$	+	++	
tricalcium aluminate	$3\text{CaO} \cdot \text{Al}_2\text{O}_3$	--	+	
gehlenite	$2\text{CaO} \cdot \text{Al}_2\text{O}_3 \cdot \text{SiO}_2$	--	+	
monocalcium ferrite	$\text{CaO} \cdot \text{Fe}_2\text{O}_3$	--	+	

\* + present, -- absent

An assessment of the physical and mechanical properties of the samples made of semi-dry pressed finely ground red mud, fired in the temperature range of 900–1100 °C, indicates their complete sintering (to zero water absorption) at a temperature of 1100 °C with the achievement of compressive strength up to 230 MPa (Fig. 6).

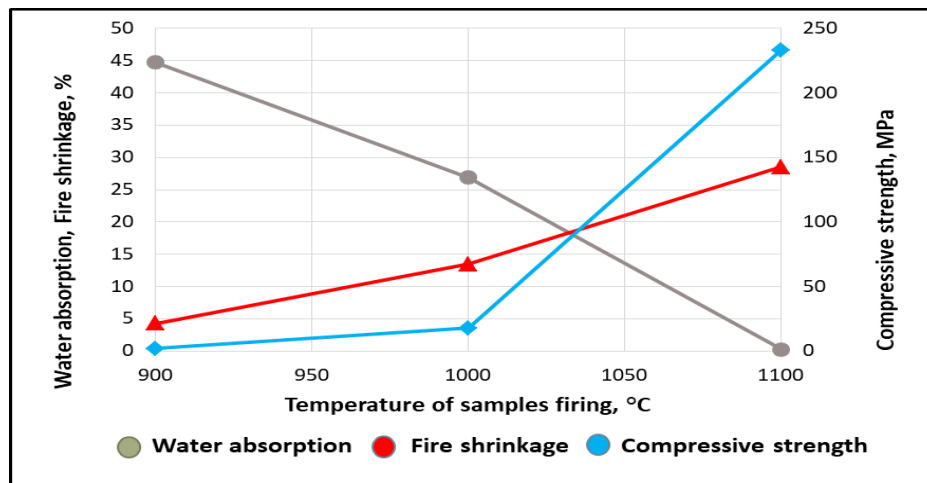


**Figure 6. Effect of heating temperature on changes in fire shrinkage, water absorption and compressive strength of the samples made of the studied red mud.**

### 3.2. Theoretical substantiation of the choice of the studied compositions "fly ash – red mud"

To predict the physical and chemical processes during heating of compositions based on the studied fly ash with the addition of red mud in an amount of 10–25 wt. %, i.e. to determine the recommended sintering interval, to establish which firing mode is required, and which phases will crystallize from the melt, a theoretical analysis of the behavior of the studied masses in the  $\text{CaO} - \text{Al}_2\text{O}_3 - \text{SiO}_2$  [41, 42],  $\text{Fe}_2\text{O}_3 - \text{Al}_2\text{O}_3 - \text{SiO}_2$  [43] and  $\text{FeO} - \text{Al}_2\text{O}_3 - \text{SiO}_2$  [41, 43] systems was carried out. These systems were chosen due to the chemical composition of the initial raw materials, namely, the predominance of silica, alumina and iron oxides in the chemical composition of the fly ash, and silica, calcium and iron oxides in the red mud. It should be noted that the studies on compositions with high-iron technogenic components (various fly ash, metallurgical sludge and slag) show that the systems with iron almost always contain both ferric ( $\text{Fe}_2\text{O}_3$ ) and ferrous iron ( $\text{FeO}$ ) [44]. This makes it necessary to consider both ternary systems with iron oxides.

For this purpose, initially the chemical compositions of the ceramic masses were calculated (Table 5).

**Table 5. Chemical composition of the investigated mixtures of fly ash with red mud in the calcined state.**

Mixture code	Content of oxides, %									Modules	
	SiO <sub>2</sub>	Al <sub>2</sub> O <sub>3</sub>	TiO <sub>2</sub>	CaO	MgO	Fe <sub>2</sub> O <sub>3</sub>	MnO	K <sub>2</sub> O	Na <sub>2</sub> O	ferric iron-alumina Fe <sub>2</sub> O <sub>3</sub> /Al <sub>2</sub> O <sub>3</sub>	calcium silicate CaO/SiO <sub>2</sub>
FA <sub>100</sub>	48.53	29.19	0.99	2.26	3.43	12.11	2.71	0.43	0.35	0.41	0.05
RM <sub>100</sub>	27.88	9.88	2.86	31.02	3.08	22.83	1.48	0.41	0.57	2.3	1.11
FA <sub>90</sub> RM <sub>10</sub>	46.47	27.26	1.17	5.14	3.39	13.18	2.59	0.43	0.37	0.48	0.12
FA <sub>85</sub> RM <sub>15</sub>	45.43	26.29	1.27	6.57	3.38	13.72	2.53	0.43	0.38	0.52	0.15
FA <sub>80</sub> RM <sub>20</sub>	44.40	25.33	1.36	8.01	3.36	14.25	2.46	0.42	0.40	0.56	0.18
FA <sub>75</sub> RM <sub>25</sub>	43.37	24.36	1.45	9.45	3.34	14.79	2.40	0.42	0.41	0.61	0.22

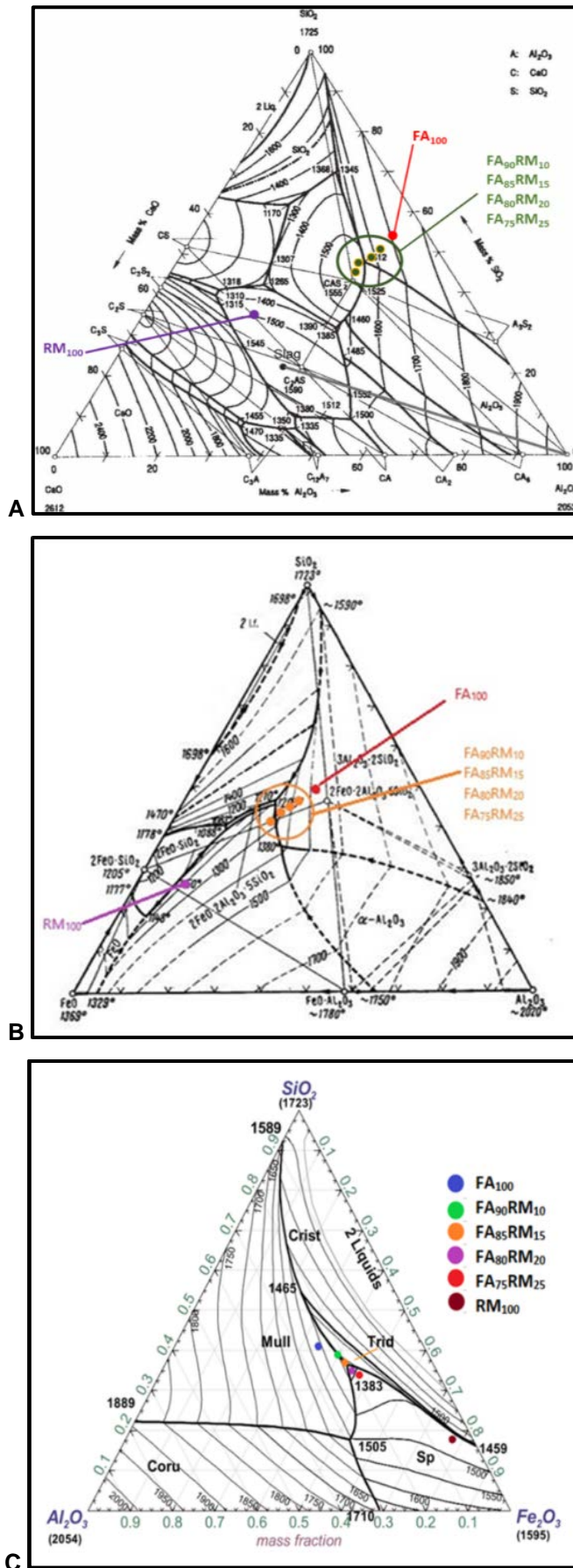
• here and below, the number in the mixture code corresponds to the content of fly ash and red mud, wt. %

The calculated chemical compositions of the studied mixtures indicate that with an increase in the addition of red mud from 10 to 25 %, the content of ferric iron oxide Fe<sub>2</sub>O<sub>3</sub> increases from 12.11 to 14.79 % (by 2.6 %) and calcium oxide CaO from 2.26 to 9.45 % (by 7 %) due to a decrease in the content of oxides SiO<sub>2</sub> (from 48.53 to 43.37 %) and Al<sub>2</sub>O<sub>3</sub> (from 29.19 to 24.36 %).

Since when red mud is added to the chemical composition of fly ash, two main oxides Fe<sub>2</sub>O<sub>3</sub> and CaO are introduced simultaneously, to assess their effect on the firing behavior of mixtures of fly ash with red mud, it was proposed to use the modules – ferric iron-alumina module (Fe<sub>2</sub>O<sub>3</sub>/Al<sub>2</sub>O<sub>3</sub>) and calcium-silicate (CaO/SiO<sub>2</sub>) module (Table 5).

Then the multicomponent chemical compositions of the studied mixtures (Table 5) were recalculated to the three-component composition CaO – Al<sub>2</sub>O<sub>3</sub> – SiO<sub>2</sub>, Fe<sub>2</sub>O<sub>3</sub> – Al<sub>2</sub>O<sub>3</sub> – SiO<sub>2</sub>, and FeO – Al<sub>2</sub>O<sub>3</sub> – SiO<sub>2</sub> according to the Richter's law of chemical equivalents [45]. For this, the three most important oxides are selected, then all oxides from the chemical composition of the studied raw materials are divided into three groups: first group – oxides of alkali and alkaline-earth metals (CaO, MgO, Na<sub>2</sub>O, K<sub>2</sub>O, etc.), second group – oxides of amphoteric metals (Al<sub>2</sub>O<sub>3</sub>, Fe<sub>2</sub>O<sub>3</sub>, etc.), third group – acid oxides (SiO<sub>2</sub>, TiO<sub>2</sub>, etc.). Within each group, the content of oxides is recalculated to the content of the most important oxide equivalent to their molecular weights. For recalculation, transition coefficients are used, derived on the basis of the Richter's law, which states that flux oxides affect the temperature according to their equivalent masses, i.e., molecular masses related to the number of cations in the formula [45].

The representative points of the calculated three-component chemical compositions of the studied mixtures were plotted on state diagrams and systems (Fig. 7); melting profiles were determined (Fig. 8).



\* The isothermal sections of the liquidus surface are given in Kelvin degrees [43]

**Figure 7. Location of studied compositions of the fly ash with red mud additions in the CaO – Al<sub>2</sub>O<sub>3</sub> – SiO<sub>2</sub> (A), FeO – Al<sub>2</sub>O<sub>3</sub> – SiO<sub>2</sub> (B) and Fe<sub>2</sub>O<sub>3</sub> – Al<sub>2</sub>O<sub>3</sub> – SiO<sub>2</sub>, (C) systems.**

To calculate the amount of melt formed in the test mixtures upon heating, it is necessary to determine, firstly, in which triangle the point of the mixture is located, and in the crystallization field of which compound the representative point of the mixture is placed. Secondly, it is necessary to build the crystallization path of the mixture composition with decreasing temperature and to calculate the amount melt according to the lever rule. Thus, if one phase decomposes into two, then the amount of substance of the resulting phases is inversely proportional to the straight line segments from the point of composition of the initial phase to the points of composition of the phases obtained [35].

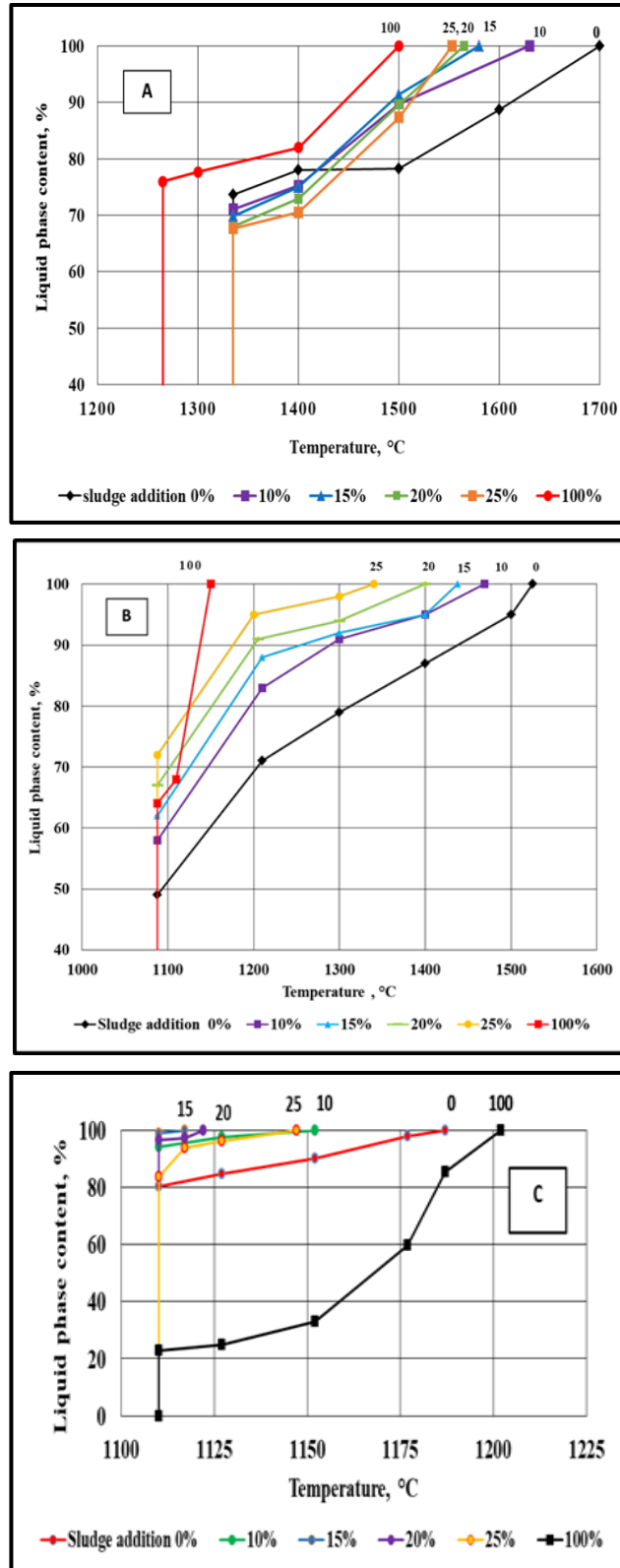


**Figure 8. Melting curves of fly ash mixtures with the addition of red mud in the CaO-Al<sub>2</sub>O<sub>3</sub>-SiO<sub>2</sub> (A), FeO-Al<sub>2</sub>O<sub>3</sub>-SiO<sub>2</sub> (B) and Fe<sub>2</sub>O<sub>3</sub>-Al<sub>2</sub>O<sub>3</sub>-SiO<sub>2</sub>, (C) systems.**

After plotting the melting profiles along the crystallization path at different temperatures, the main characteristics of the melts formed in the studied compositions upon heating were determined (Table 6–8).

**Table 6. Chemical compositions and characteristics of the study mixtures in the CaO – Al<sub>2</sub>O<sub>3</sub> – SiO<sub>2</sub> system.**

Mixture code	Oxide content, wt.%,			Characteristics of the eutectic phase			Complete melting temperature, °C
	SiO <sub>2</sub>	Al <sub>2</sub> O <sub>3</sub>	CaO	Temperature, °C	Eutectic melt content, %	Crystalline phase content, %	
FA <sub>100</sub>	51.35	38.47	10.19	1335	74	26	1700
RM <sub>100</sub>	32.74	26.64	40.62	1265	76	24	1500
FA <sub>90</sub> RM <sub>10</sub>	49.56	37.33	13.11	1335	71	29	1667
FA <sub>85</sub> RM <sub>15</sub>	48.66	36.76	14.58	1335	70	30	1580
FA <sub>80</sub> RM <sub>20</sub>	47.76	36.19	16.06	1335	68	32	1565
FA <sub>75</sub> RM <sub>25</sub>	46.85	35.61	17.54	1335	68	32	1553

Characteristics of the resulting melts in (RM100) is the component of the ternary eutectic with the lowest temperature (1265 °C). Therefore, in the compositions of the studied ceramic masses, it should be the first to melt and to promote sintering of fly ash based samples (FA<sub>100</sub>), which is a component of the ternary eutectic with a temperature of 1335 °C. However, as it was found, the addition of 10 to 25 % of red mud to the fly ash not only does not reduce the temperature of the appearance of eutectic melts, but even increases the total content of the crystalline phase at temperatures up to 1400 °C (Fig. 9).

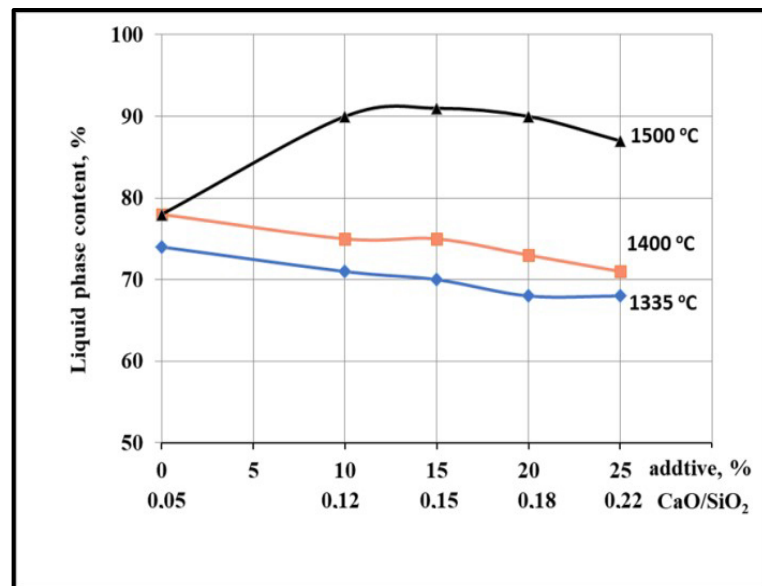


**Figure 9. Influence of the composition of fly ash with red mud additives (10–25 %) mixtures on the formation of a melt during heating in the CaO – Al<sub>2</sub>O<sub>3</sub> – SiO<sub>2</sub> system.**

Thus, the calcium silicate module can be associated with the formation of a crystalline part during firing of the fly ash and red mud mixtures used.

A theoretical consideration of the behavior of the studied compositions upon heating in the ternary systems with iron oxides FeO – Al<sub>2</sub>O<sub>3</sub> – SiO<sub>2</sub> and Fe<sub>2</sub>O<sub>3</sub> – Al<sub>2</sub>O<sub>3</sub> – SiO<sub>2</sub>, indicates that the appearance of eutectic melt during heating of all compositions occurs at the same temperature of 1088 °C (in FeO – Al<sub>2</sub>O<sub>3</sub> – SiO<sub>2</sub> system) and at 1110 °C (in Fe<sub>2</sub>O<sub>3</sub> – Al<sub>2</sub>O<sub>3</sub> – SiO<sub>2</sub>, system), regardless of the presence of red mud additives in the fly ash (Table 7, 8).

**Table 7. Chemical compositions and characteristics of the study mixtures in the FeO – Al<sub>2</sub>O<sub>3</sub> – SiO<sub>2</sub> system.**

Mixture code	Oxide content, wt. %			Characteristics of the eutectic phase			Complete melting temperature, °C
	SiO <sub>2</sub>	Al <sub>2</sub> O <sub>3</sub>	FeO	Temperature, °C	Eutectic melt content, %	Crystalline phase content, %	
FA <sub>100</sub>	48.34	28.64	23.02	1088	49	51	1525
RM <sub>100</sub>	27.71	9.12	63.17	1088	64	36	1150
FA <sub>90</sub> RM <sub>10</sub>	46.16	26.58	27.26	1088	58	42	1469
FA <sub>85</sub> RM <sub>15</sub>	45.08	25.56	29.36	1088	62	38	1438
FA <sub>80</sub> RM <sub>20</sub>	44.01	24.54	31.45	1088	67	33	1400
FA <sub>75</sub> RM <sub>25</sub>	42.94	23.53	33.53	1088	72	28	1340

**Table 8. Chemical compositions and characteristics of the study mixtures in the Fe<sub>2</sub>O<sub>3</sub> – Al<sub>2</sub>O<sub>3</sub> – SiO<sub>2</sub>, system.**

Mixture code	Oxide content, wt. %			Characteristics of the eutectic phase			Complete melting temperature, °C
	SiO <sub>2</sub>	Al <sub>2</sub> O <sub>3</sub>	Fe <sub>2</sub> O <sub>3</sub>	Temperature, °C	Eutectic melt content, %	Crystalline phase content, %	
FA <sub>100</sub>	41.64	24.67	33.69	1110	80	20	1187
RM <sub>100</sub>	17.79	5.85	76.35	1110	23	77	1202
FA <sub>90</sub> RM <sub>10</sub>	38.38	22.09	39.53	1110	94	6	1152
FA <sub>85</sub> RM <sub>15</sub>	36.85	20.89	42.27	1110	95	5	1117
FA <sub>80</sub> RM <sub>20</sub>	35.37	19.72	44.90	1110	96	4	1122
FA <sub>75</sub> RM <sub>25</sub>	33.96	18.61	47.44	1110	84	16	1147

We compared the data obtained on the effect of iron oxides on the processes during heating in the studied mixtures of fly ash with red mud additives. It indicates the fluxing effect of both types of iron oxides introduced with red mud, regardless of their form – ferric (Fe<sub>2</sub>O<sub>3</sub>) or ferrous iron (FeO). At the same time, ferric iron has a more active effect in these mixtures than ferrous iron.

It was established that the addition of 10 to 25 % bauxite sludge into the initial aluminosilicate fly ash with its own high content of iron oxide impurities (Table 1) provides an increase in the content of the eutectic melt on average from 9 % to 23 % depending on the composition of the mixture. In addition, a comparative analysis of the melting curves (Fig. 8, B, C) indicates that, in order to ensure liquid-phase sintering of the samples from the compositions under consideration, it is necessary to use a firing temperature below 1100 °C. The continuous increase in the amount of melt in the entire range of temperatures under consideration up to complete melting (Fig. 10) is due to the fluxing effect of iron oxides introduced with high-iron red mud on the formation of a liquid phase when such compositions are heated.

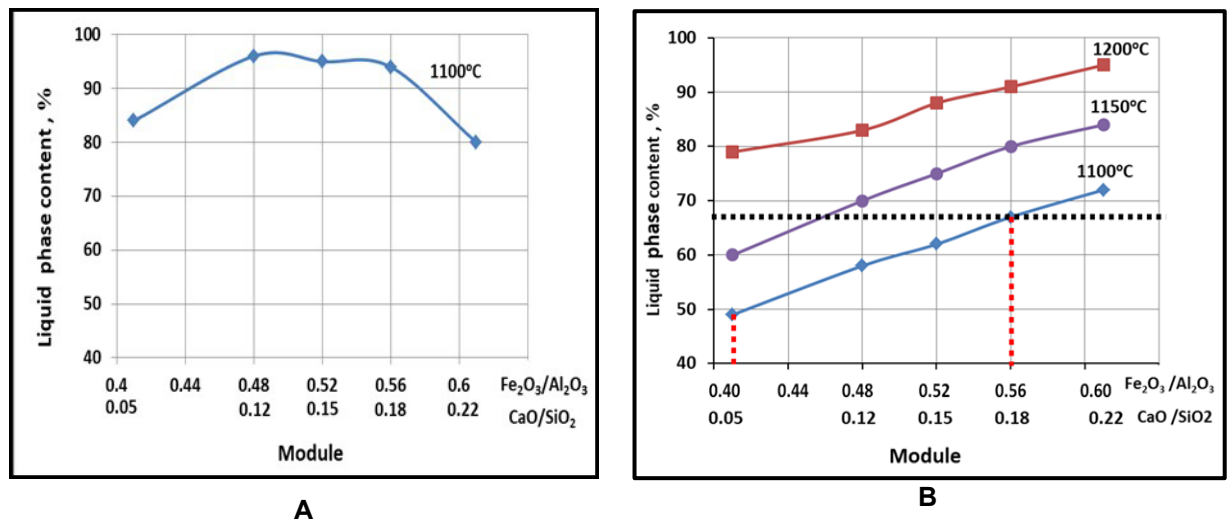


**Figure 10. Influence of the composition of fly ash with red mud additives (10–25 %) mixtures on the formation of a melt during heating in Fe<sub>2</sub>O<sub>3</sub> - Al<sub>2</sub>O<sub>3</sub> - SiO<sub>2</sub>, (A) and FeO - Al<sub>2</sub>O<sub>3</sub> - SiO<sub>2</sub> (B) systems.**

Thus, the predictive analysis of the behavior of fly ash compositions with the addition of bauxite sludge in CaO - Al<sub>2</sub>O<sub>3</sub> - SiO<sub>2</sub>, FeO - Al<sub>2</sub>O<sub>3</sub> - SiO<sub>2</sub> and Fe<sub>2</sub>O<sub>3</sub> - Al<sub>2</sub>O<sub>3</sub> - SiO<sub>2</sub>, systems allowed us to:

- identify the fluxing effect of red mud additives on the fly ash under study;
- determine the optimal firing temperatures for the samples from the analyzed compositions – 1100 °C, at which no more than 65–68 % melt is formed in the samples. An increase of temperature above 1100 °C will theoretically cause the phenomena of melting and deformation of products under the weight of their own mass.
- ensure densely sintered mullite-anorthite ceramics; the raw mixtures of aluminosilicate fly ash with red mud should have a composition with Fe<sub>2</sub>O<sub>3</sub>/Al<sub>2</sub>O<sub>3</sub> module equal to 0.4–0.56 and CaO/SiO<sub>2</sub> module equal to 0.07–0.18.

### 3.3. The effect of red mud additives on the sample sintering from fly ash by semi-dry pressing

It was established that at firing temperatures of 1100–1200 °C the samples of semi-dry pressing from fly ash without additives (FA<sub>100</sub>) are characterized by high porosity (with water absorption of 19–26 %) and low compressive strength (from 3 to 37.9 MPa) depending on the firing temperature (Fig. 11).

The introduction of the red mud additives activates the sintering of samples at 1150–1200 °C: water absorption decreases from 26 % in the case of fly ash sample without additive (FA<sub>100</sub>) to 22 % in the case of samples from fly ash mixture with 10 % red mud additive (FA<sub>90</sub>RM<sub>10</sub>), while the compressive strength increases from 3 to 20 MPa. Higher temperature heating up to 1200 °C ensures the preservation of the general indicated trend.

Further increase in the content of red mud from 10 to 15 % in mixtures (FA<sub>85</sub>RM<sub>15</sub>) activates the process of sintering and hardening of samples even more, providing a decrease in the water absorption of samples from 26 to 2 % and an increase in compressive strength from 3 to 170 MPa at a temperature of 1200 °C.

Thus, when designing the compositions of ceramic masses for the production of high-strength ceramics, it is necessary to focus on the established criteria for activating the sintering process of compositions of aluminosilicate fly ash with red mud additives: the composition of the mixture (according to the value of ferric iron-alumina Fe<sub>2</sub>O<sub>3</sub>/Al<sub>2</sub>O<sub>3</sub> and calcium silicate CaO/SiO<sub>2</sub> modules) and the optimal firing temperature of the samples (Fig. 12).

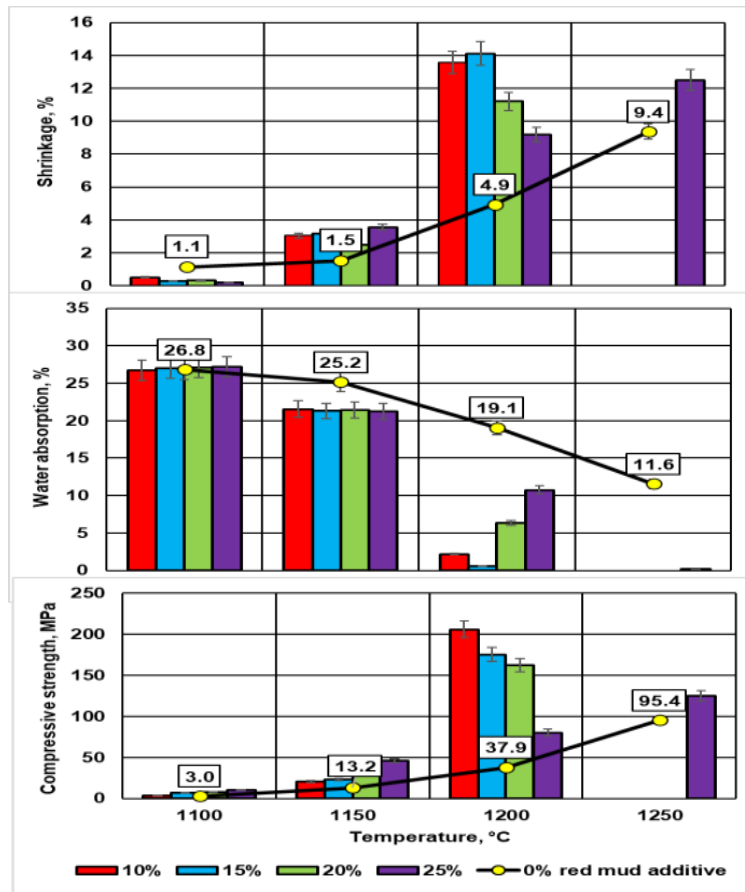


Figure 11. Influence of red mud additive (10–25 % wt.) on the physical and mechanical properties of samples of semi-dry pressing from fly ash, fired at 1100–1250 °C.

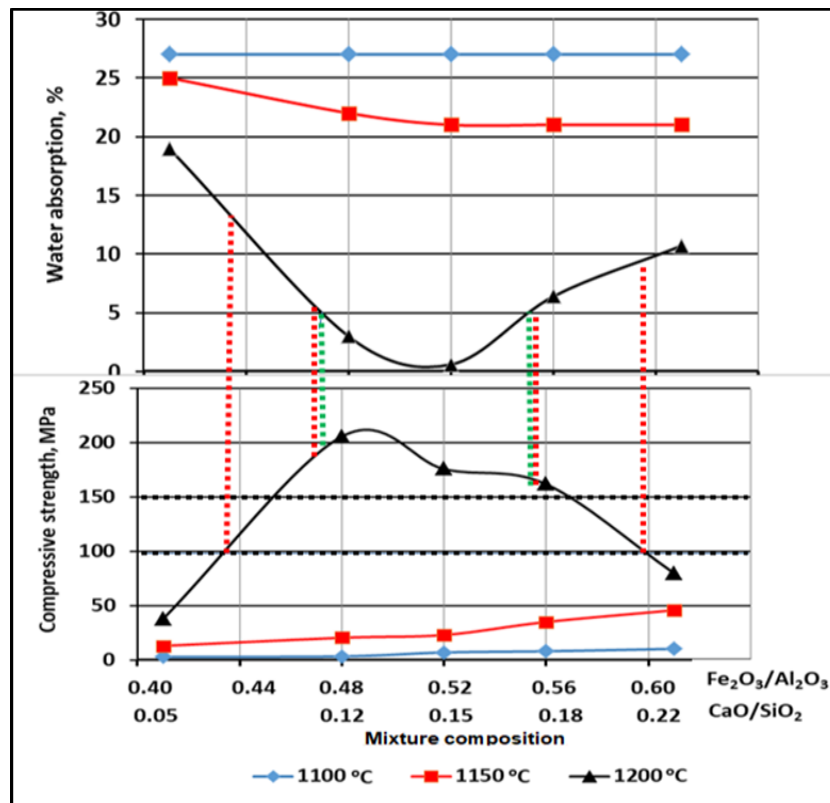


Figure 12. Influence of the composition of fly ash with red mud mixtures on the physical and mechanical properties of samples fired at 1100–1200 °C: (green dotted lines indicate the range of mixture compositions for densely sintered ceramics, red dotted lines – for porous ceramics)



For example, to obtain sintered ceramics (with water absorption less than 5 %) with a compressive strength of at least 150 MPa, it is necessary to use mixtures with  $\text{Fe}_2\text{O}_3/\text{Al}_2\text{O}_3$  module equal to 0.47–0.55 and  $\text{CaO}/\text{SiO}_2$  module equal to 0.11–0.17, and firing of the samples is carried out at a temperature of 1200 °C (green dotted line). To obtain porous ceramics at 1200 °C (with water absorption of more than 5 %) with a compressive strength of more than 100 MPa, it is necessary to use mixtures of two types: 1) with  $\text{Fe}_2\text{O}_3/\text{Al}_2\text{O}_3$  module equal to 0.43–0.47,  $\text{CaO}/\text{SiO}_2$  module equal to 0.08–0.11 and 2) with  $\text{Fe}_2\text{O}_3/\text{Al}_2\text{O}_3$  module equal to 0.55–0.60,  $\text{CaO}/\text{SiO}_2$  module equal to 0.17–0.22 (red dotted line).

The explanation for the processes of formation of these technological properties should be sought in the physical and chemical processes that occur during the firing of these compositions. For this, the phase composition of the investigated mixtures after their heat treatment was studied by the X-ray method.

The obtained X-ray diffraction patterns indicate that, depending on the composition of the fly ash and red mud mixtures and the temperature regime of firing, the main crystalline phases are mullite, anorthite and cristobalite.

It was found that in the absence of red mud additions, the fly ash heating at temperatures of 1100–1200 °C had practically no effect on quantitative changes in the content of the minerals that make up the fly ash. However, in the presence of 10–20 % red mud additives, a decrease in the intensity of mullite and cristobalite X-ray reflections and a significant increase in anorthite reflections are observed, regardless of the firing temperature (Fig. 13).

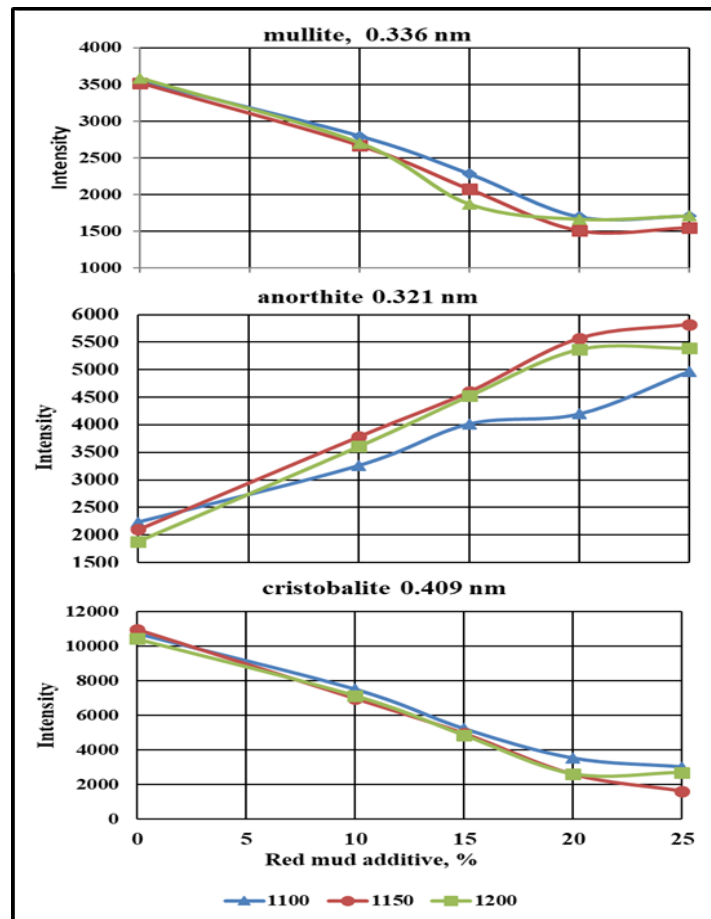


**Figure 13. Influence of the red mud additives (10–25 %) on the formation of the phase composition of samples from fly ash fired at 1100–1200 °C.**

An increase in the intensity of anorthite X-ray reflections in fired samples from fly ash – red mud mixtures up to 2.5–3 times (depending on the content of the additive and the firing temperature) while reducing the content of mullite up to 2 times and cristobalite – up to 2 times is associated with solid-phase synthesis of anorthite at temperatures 1100–1200 °C according to the reaction:



*mullite*                      *cristobalite*                      *anorthite*

Thus, the resulting product made from researched compositions of fly ash with bauxite sludge are anorthite ceramics. The  $\text{CaO}/\text{SiO}_2$  module equal to 0.12–0.22 is responsible for the formation of the crystalline phase (anorthite) during the firing of samples from a mixture of fly ash with red mud additives.

The formation of anorthite in samples from mixtures of clay with red mud at a temperature of 1000–1100 °C was recorded in [46].

Recently, a few studies have investigated the effect of the  $\text{CaO}/\text{SiO}_2$  ratio on the phase crystallization and properties of sintered materials based on anorthite. Overall, these studies have been focusing on the use of industrial wastes combined with natural resources [47, 48]. Tabit et al. [49] found that an increase in the  $\text{CaO}/\text{SiO}_2$  ratio from 0.12–0.8 in mixtures of coal fly ash and ladle furnace slag promoted crystallization of anorthite as the main phase which is consistent with the results obtained in this study.

The studies carried out make it possible to determine the optimal compositions and technological modes for obtaining ceramics based on the studied raw materials in comparison with the properties of ash samples without the addition of red mud FA<sub>100</sub> (Table 8).

**Table 8. Optimum compositions, technological conditions and properties of ceramics based on fly ash with the studied red mud.**

Composition code	Component composition, %		Temperature, °C			Ceramic properties		
			calcination of raw materials		firing of samples			
	fly ash	red mud	fly ash	red mud		shrinkage %	water absorption, %	compressive strength, MPa
FA <sub>100</sub>	100	0	1200	–	1250	9.4	11.6	95.4
FA <sub>90</sub> RM <sub>10</sub>	90	10				13.6	2.2	206.2
FA <sub>85</sub> RM <sub>15</sub>	85	15	1200	1000	1200	14.1	0.6	175.5
FA <sub>80</sub> RM <sub>20</sub>	80	20				11.2	6.4	162.4

The previously stated hypothesis about the fluxing effect of bauxite sludge additives on the sintering of the fly ash based samples was confirmed by a change in the physical and mechanical properties of samples from these compositions, as well as by electron microscopy (Fig. 14).

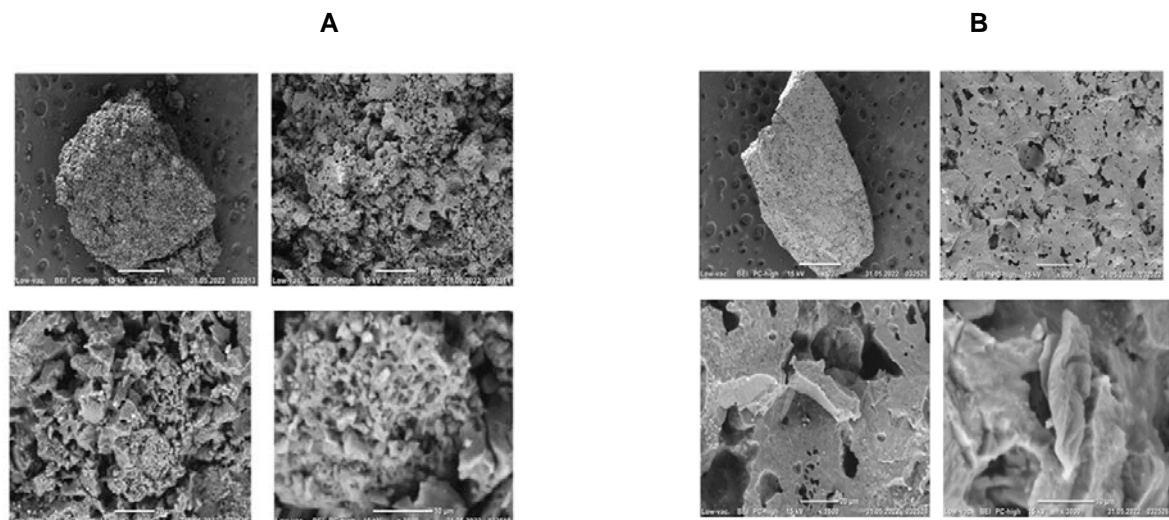


**Figure 14. Electron micrographs of semi-dry pressed samples, fired at 1200 °C, from ash without red mud (A) and with addition of 10% red mud (B).**

In particular, microscopic images of calcined fly ash without red mud additives show that the sample is a loosely sintered material consisting of individual finely porous aggregates separated from each other by deep winding pores. The introduction of red mud additive in an amount of 10 % sharply activates the process of liquid-phase sintering of samples from fly ash due to red mud melting [50, 51] at 1150 °C, which leads to the formation of a monolithic structure with internal pores approaching a sphere in shape.

## 4. Conclusion

The following results were obtained upon the completed experimental studies:

1. The chemical composition, mineralogical (phase) composition, structural features of the initial technogenic raw materials and their changes during heating were established. The studied fly ash was a variety of aluminosilicate fly ash with a low content of calcium oxide (2.26 % CaO) and a high content of aluminum oxide (29.19 % Al<sub>2</sub>O<sub>3</sub>) and iron oxide (12.11 % Fe<sub>2</sub>O<sub>3</sub>). The content of residual fuel was not more than 2.5 %, the crystalline part of which was composed of mullite, quartz and ferruginous mineral in the form of hematite, with a full sintering temperature (up to water absorption of not more than 5 %) above 1300 °C. Bauxite sludge (red mud) in terms of chemical composition was represented mainly by oxides of silica (21.03 % SiO<sub>2</sub>), calcium (23.46 % CaO), iron (17.27 % Fe<sub>2</sub>O<sub>3</sub>) and aluminum (7.47 % Al<sub>2</sub>O<sub>3</sub>). In terms of mineralogical composition, it was composed of calcite, hydrated calcium silicates and aluminates, hematite and magnetite, fully sintered at 1100 °C.

2. Theoretical analysis of the behavior of ash compositions with the addition of bauxite sludge (10–25 %) made it possible to reveal the fluxing effect of bauxite sludge additions to the studied fly ash. To determine the optimal firing temperatures for samples from the analyzed compositions (1100–1150 °C), to ensure a densely sintered mullite-anorthite ceramics, the raw mixtures of aluminosilicate fly ash with red mud should have a composition with Fe<sub>2</sub>O<sub>3</sub>/Al<sub>2</sub>O<sub>3</sub> module equal to 0.4–0.54 and CaO/SiO<sub>2</sub> module equal to 0.07–0.17.

3. Theoretical predictions were confirmed by experimental studies. We proved that the resulting ceramics from the investigated compositions of fly ash with bauxite sludge (10–25 %) were mullite-anorthite ceramics. High compressive strength (up to 210 MPa) of the samples from the recommended compositions of fly ash with 10–20 % red mud are promising for further testing in the technology of densely sintered wear-resistant ceramic materials (building clinker ceramics, ceramic proppants and others) with water absorption of 0.5–2 %, and compressive strength up to 175–200 MPa.

## References

1. Archambo, M., Kawatra, S.K. Red Mud: Fundamentals and new avenues for utilization. *Mineral Processing and Extractive Metallurgy Review*. 2021. 42(7). Pp. 427–450. DOI: 10.1080/08827508.2020.1781109
2. Li, R., Zhang, T., Liu, Y., Li, G., Xie, L. Calcification–carbonation method for red mud processing. *Journal of Hazardous Materials*. 2016. 316. Pp. 94–101. DOI: 10.1016/j.jhazmat.2016.04.072
3. Liu, S., Guan, X., Zhang, S., Dou, Z., Feng, C., Zhang, H., Luo, S. Sintered bayer red mud based ceramic bricks: Microstructure evolution and alkalis immobilization mechanism. *Ceramics International*. 2017. 43(15). Pp. 13004–13008. DOI: 10.1016/j.ceramint.2017.07.036
4. Hou, L., Liu, T., Lu, A. Red mud and fly ash-based ceramic foams using starch and manganese dioxide as foaming agent. *Transactions of Nonferrous Metals Society of China*. 2017. 27(3). Pp. 591–598. DOI: 10.1016/S1003-6326(17)60066-9
5. Paramguru, R.K., Rath, P.C., Misra, V.N. Trends in red mud utilization – a review. *Mineral Processing and Extractive Metallurgy Review*. 2006. 26(1). Pp. 1–29. DOI: 10.1080/08827500490477603
6. Kavas, T. Use of boron waste as a fluxing agent in production of red mud brick. *Building and Environment*. 2006. 41(12). Pp. 1779–1783. DOI: 10.1016/j.buildenv.2005.07.019
7. Lopesa, D.V., Durana, E., Cesconeto, F.R., Almeida, P.V., Kovalevsky, A.V., Quina, M.J., Frade, J.R. Direct processing of cellular ceramics from a single red mud precursor. *Ceramics International*. 2020. 46(10) Pp. 16700–16707. DOI: 10.1016/j.ceramint.2020.03.244
8. Muraleedharan, M., Nadir, Y. Factors affecting the mechanical properties and microstructure of geopolymers from red mud and granite waste powder: A review. *Ceramics International*. 2021. 47(10). Pp. 13257–13279. DOI: 10.1016/j.ceramint.2021.02.009
9. Xia, F., Cui, S., Pu, X. Performance study of foam ceramics prepared by direct foaming method using red mud and K-feldspar washed waste. *Ceramics International*. 2022. 48(4). Pp. 5197–5203. DOI: 10.1016/j.ceramint.2021.11.059
10. Alekseev, K., Mymrin, V., Avanci, M. A., Klitzke, W., Magalhães, W. L.E., Silva, P.R., Catai, R.E., Silva, D.A., Ferraz, F.A. Environmentally clean construction materials from hazardous bauxite waste red mud and spent foundry sand. *Construction and Building Materials*. 2019. 116860. DOI: 10.1016/j.conbuildmat.2019.116860
11. Sglavo, V.M., Camprostrini, R., Maurina, S., Carturan, G., Monagheddu, M., Budroni, G., Cocco, G. Bauxite 'red mud' in the ceramic industry. Part 1: thermal behavior. *Journal of the European Ceramic Society*. 2000. 20(3). Pp. 235–244. DOI: 10.1016/S0955-2219(99)00088-6
12. Sglavo, V.M., Maurina, S., Conci, A., Salviati, A., Carturan, G., Cocco, G. Bauxite 'red mud' in the ceramic industry. Part 2: production of clay-based ceramics. *Journal of the European Ceramic Society*. 2000. 20(3). Pp. 245–252. DOI: 10.1016/S0955-2219(99)00156-9
13. Yao, Z.T., Ji, X.S., Sarker, P.K., Tang, J.H., Ge, L.Q., Xia, M.S., Xi, Y.Q. A comprehensive review on the applications of coal fly ash. *Earth-Science Reviews*. 2015. 141. Pp. 105–121. DOI: 10.1016/j.earscirev.2014.11.016
14. Blissett, R.S., Rowson, N.A. A review of the multi-component utilization of coal fly ash. *Fuel*. 2012. 97. Pp. 1–23. DOI: 10.1016/j.fuel.2012.03.024
15. Ma, B., Qi, M., Peng, J., Li, Z. The compositions, surface texture, absorption, and binding properties of fly ash in China. *Environment International*. 1999. 25(4). Pp. 423–432 DOI: 10.1016/S0160-4120(99)00010-0
16. Vassilev, S.V., Vassileva, C.G. Geochemistry of coals, coal ashes and combustion wastes from coal-fired power stations. *Fuel Processing Technology*. 1997. 51. Pp. 19–45. DOI: 10.1016/S0378-3820(96)01082-X

17. Vassilev, S.V., Menendez, R., Alvarez, D., Dias-Somoano, M., Martinez-Tarazona, M.R. Phase-mineral and chemical composition of coal fly ashes as a basis for their multicomponent utilization. 1. Characterization of feed coals and fly ashes. *Fuel*. 2003. 82(14). Pp. 1793–1811. DOI: 10.1016/S0016-2361(03)00123-6
18. Leiva, C., Rodriguez-Galán, M., Arenas, C., Alonso-Fariñas, B., Peceño, B. A mechanical, leaching and radiological assessment of fired bricks with a high content of fly ash. *Ceramics International*. 2018. 44(11). Pp. 13313–13319. DOI: 10.1016/j.ceramint.2018.04.162
19. Mi, H., Yi, L., Wu, Q., Xia, J., Zhang, B. Preparation of high-strength ceramsite from red mud, fly ash, and bentonite. *Ceramics International*. 2021. 47(13). Pp. 18218–18229. DOI: 10.1016/j.ceramint.2021.03.141
20. Horiuchi, S., Kawaguchi, M., Yasuhara, K. Effective use of fly ash slurry as fill material. *Journal of Hazardous Materials*. 2000. 76(2–3). Pp. 301–337. DOI: 10.1016/S0304-3894(00)00205-3
21. Vakalova, T.V., Khabas, T.A., Revva, I.B., Pavlova, I.A. Heat-insulating ceramics which have a nanoporous structure and are made with the use of ash-bearing wastes from power plants. *Refractories and Industrial Ceramic*. 2015. 55. Pp. 505–510. DOI: 10.1007/s11148-015-9754-z
22. Vakalova, T.V., Revva, I.B. Highly porous building ceramics based on «clay-ash microspheres» and «zeolite-ash microspheres» mixtures. *Construction and Building Materials*. 2022. 317. 125922. DOI: 10.1016/j.conbuildmat.2021.125922
23. Vereshchagin, V.I., Pogrebenkov, V.M., Vakalova, T.V. Utilization of natural and technogenous raw materials of Siberian region in production of the building ceramics and thermal insulating materials. *Stroitel'nye Materials*. 2004. 2. Pp. 28–32. View Record in Scopus Google Scholar.
24. Park, Y.M., Yang, T.Y., Yoon, S.Y., Stevens, R., Park, H.C. Mullite whiskers derived from coal fly ash. *Materials Science and Engineering: A*. 2007. 454–455. Pp. 518–522. DOI: 10.1016/j.msea.2006.11.114
25. Wu, X., Huo, Z., Ren, Q., Li, H., Lin, F., Wei, T. Preparation and characterization of ceramic proppants with low density and high strength using fly ash. *Journal of Alloys and Compounds*. 2017. 702. Pp. 442–448. DOI: 10.1016/j.jallcom.2017.01.262
26. Ma, B.Y., Su, C., Ren, X., Gao, Z., Qian, F., Yang, W., Liu, G., Li, H., Yu, J., Zhu, Q. Preparation and properties of porous mullite ceramics with high-closed porosity and high strength from fly ash via reaction synthesis process. *Journal of Alloys and Compounds*. 2019. 803. Pp. 981–991. DOI: 10.1016/j.jallcom.2019.06.272
27. Lin, B., Li, S., Hou, X., Li, H. Preparation of high performance mullite ceramics from high-aluminum fly ash by an effective method. *Journal of Alloys and Compounds*. 2015. 623. Pp. 359–361. DOI: 10.1016/j.jallcom.2014.11.023
28. He, Y., Cheng, W., Cai, H. Characterization of  $\alpha$ -cordierite glass-ceramics from fly ash. *Journal of Hazardous Materials*. 2005. 120 (1–3). Pp. 265–269. DOI: 10.1016/j.jhazmat.2004.10.028
29. Hui, T., Sun, H.J., Peng T.J. Preparation and characterization of cordierite-based ceramic foams with permeable property from asbestos tailings and coal fly ash. *Journal of Alloys and Compounds*. 2021. 885. 160967. DOI: 10.1016/j.jallcom.2021.160967
30. Zong, Y., Wan, Q., Cang, D. Preparation of anorthite-based porous ceramics using high-alumina fly ash microbeads and steel slag. *Ceramics International*. 2019. 45(17). Pp. 22445–22451. DOI: 10.1016/j.ceramint.2019.08.003
31. Tabit, K., Hajjou, H., Waqif, M., Saâdi, L. Effect of CaO/SiO<sub>2</sub> ratio on phase transformation and properties of anorthite-based ceramics from coal fly ash and steel slag. *Ceramics International*. 2020. 46(6). Pp. 7550–7558. DOI: 10.1016/j.ceramint.2019.11.254
32. Ma, B.Y., Ren, X., Yin, Y., Yuan, L., Zhang, Z., Li, Z., Li, G., Zhu, Q., Yu, J. Effects of processing parameters and rare earths additions on preparation of Al<sub>2</sub>O<sub>3</sub>-SiC composite powders from coal ash. *Ceramics International*. 2017. 43(15). Pp. 11830–11837. DOI: 10.1016/j.ceramint.2017.05.362
33. Ma, B.Y., Li, Y., Cui, S.G., Zhai, Y.C. Preparation and sintering properties of zirconia–mullite–corundum composites using fly ash and zircon. *Transactions of Nonferrous Metals Society of China*. 2010. 20(12). Pp. 2331–2335. DOI: 10.1016/S1003-6326(10)60650-4
34. Shih, W.H., Chang, H.L. Conversion of fly ash into zeolites for ion-exchange applications. *Materials Letters*. 1996. 28 (4–6). Pp. 263–268. DOI: 10.1016/0167-577X(96)00064-X
35. Kingery, W.D., Bowen, H.K., Uhlmann, D.N. *Introduction to Ceramics*. John Wiley & Sons, Inc. 1976. 1032 p.
36. Kaya, C., Butler, E.G., Selcuk, A., Boccaccini, A.R., Lewis, M.H. Mullite (NextelTM720) fibre-reinforced mullite matrix composites exhibiting favourable thermomechanical properties. *Journal of the European Ceramic Society*. 2002. 22. Pp. 2333–2342. DOI: 10.1016/S0955-2219(01)00531-3
37. Chen, X., Li, T., Ren, Q., Wu, X., Li, H., Dang, A., Zhao, Z., Shang, Y., Zhang, Y. Mullite whisker network reinforced ceramic with high strength and lightweight. *Journal of Alloys and Compounds*. 2017. 700. Pp. 37–42.
38. German, R.M., Suri, P., Park, S.J. Review: liquid phase sintering. *Journal of Materials Science*. 2009. 44. Pp 1–39. DOI: 10.1007/s10853-008-3008-0
39. Vakalova, T.V., Reshetova, A.A., Revva, I.B., Rusinov, P.G., Balamygin, D.I. Effect of thermochemical activation of clay raw materials on phase formation, microstructure and properties of aluminosilicate proppants. *Applied Clay Science*. 2019. 183. 105335. DOI: 10.1016/j.clay.2019.105335
40. Pontikes, Y., Rathossi, C., Nikolopoulos, P., Angelopoulos, G.N., Jayaseelan, D.D., Lee, W.E. Effect of firing temperature and atmosphere on sintering of ceramics made from Bayer process bauxite residue. *Ceramics International*. 2009. 35 (1). Pp. 401–407. DOI: 10.1016/j.ceramint.2007.11.013
41. Toropov, N.A., Barzakovsky, V.P. et al. Diagrams of state of silicate systems (In Russian). 1972. 448 p.
42. Deckerov, S.A., Kang, Y.B., Jung, I.H. Thermodynamic Database for the Al-Ca-Co-Cr-Fe-Mg-Mn-Ni-Si-O-P-S System and Applications in Ferrous Process Metallurgy. *Journal of Phase Equilibria and Diffusion*. 2009. 30 (5). Pp. 443–461. DOI: 10.1007/s11669-009-9569-z
43. Prostavka, V., Shishin, D., Shevchenko, M., Jak, E. Thermodynamic optimization of the Al<sub>2</sub>O<sub>3</sub>-FeO-Fe<sub>2</sub>O<sub>3</sub>-SiO<sub>2</sub> oxide system. *Calphad*. 2019. 67. DOI: 10.1016/j.calphad.2019.101680
44. Jak, E., Degterov, S., Pelton, A.D., Happ, J., Hayes, P.C.: in: R.P.Gupta, T.F.Wall, L.Baxter (Eds.) *Thermodynamic modelling of the system Al<sub>2</sub>O<sub>3</sub>-SiO<sub>2</sub>-CaO-FeO-Fe<sub>2</sub>O<sub>3</sub> to characterise coal ash slags, The Impact of Mineral Impurities in Solid Fuel Combustion*. Kluwer Academic/Plenum Publishers, New York, N.Y., USA, 1999. 723. DOI: 10.1007/0-306-46920-0\_55
45. Zemlyanoy, K.G., Pavlova, I.A. Phase equilibria in oxide systems (In Russian). 2021. 228 p.

46. Pérez-Villarejo, L., Corpas-Iglesias, F.A., Martínez-Martínez, S., Artiaga, R., Pascual-Cosp, J. Manufacturing new ceramic materials from clay and red mud derived. *Construction and Building Materials*. 2012. 35. Pp 656–665. DOI: 10.1016/j.conbuildmat.2012.04.133
47. Li, B.W., Chen, H., Zhao, M., Zhang, X.F., Du, Y.S., Deng, L.B. Effect of CaO/SiO<sub>2</sub> ratio and TiO<sub>2</sub> on glass-ceramics made from steel slag and fly ash. *Applied Mechanics and Materials*. 2012. 217–219. Pp. 119–123. DOI:10.4028/www.scientific.net/AM
48. Yang, Z., Lin, Q., Lu, S., He, Y., Liao, G., Ke, Y. Effect of CaO/SiO<sub>2</sub> ratio on the preparation and crystallization of glass-ceramics from copper slag. *Ceramics International*. 2014. 40. Pp. 7297–7305. DOI: 10.1016/j.ceramint.2013.12.071
49. Tabit, K., Hajjou, H., Waqif, M., Saâdi, L. Effect of CaO/SiO<sub>2</sub> ratio on phase transformation and properties of anorthite-based ceramics from coal fly ash and steel slag. *Ceramics International*. 2020. 46(6). Pp. 7550–7558. DOI: 10.1016/j.ceramint.2019.11.254
50. Pei, D., Li, Y., Cang, D. In situ XRD study on sintering mechanism of SiO<sub>2</sub>-Al<sub>2</sub>O<sub>3</sub>-CaO-MgO ceramics from red mud. *Materials Letters*. 2019. 240. Pp. 229–232. DOI: 10.1016/j.matlet.2019.01.019
51. Ren, Y., Ren, Q., Wu, X., Zheng, J., Hai, O. Mechanism of low temperature sintered high-strength ferric-rich ceramics using bauxite tailings. *Materials Chemistry and Physics*. 2019. 238. Pp. 121929. DOI: 10.1016/j.matchemphys.2019.121929

**Information about authors:**

**Tatiana Vakalova**, Doctor of Technical Sciences

ORCID: <https://orcid.org/0000-0002-1756-3526>

E-mail: [tvv@tpu.ru](mailto:tvv@tpu.ru)

**Nikolay Sergeev**,

ORCID: <https://orcid.org/0000-0002-7656-5628>

E-mail: [axioma-13@yandex.ru](mailto:axioma-13@yandex.ru)

**Dias Tolegenov**,

ORCID: <https://orcid.org/0000-0001-8242-0655>

E-mail: [www.dika-92@mail.ru](mailto:www.dika-92@mail.ru)

**Diana Tolegenova**,

E-mail: [diana\\_donj@mail.ru](mailto:diana_donj@mail.ru)

Received 01.11.2022. Approved after reviewing 22.05.2023. Accepted 27.05.2023.